Title: pH-dependent beta-lactam resistance in *Klebsiella pneumoniae* is mediated by paralogous class B PBPs and the class A PBP, PBP1b.

Authors

Sarah Beagle[1] and Petra Anne Levin[1*]

Affiliations

[1]Washington University in St. Louis, Department of Biology, St. Louis, Missouri, USA

*Correspondence: plevin@wustl.edu

Abstract

Klebsiella pneumoniae is a leading cause of global deaths due to antibiotic resistance. Of particular concern is the rapid expansion of resistance to beta-lactam antibiotics within *K. pneumoniae* lineages. The environmental factors that influence pathogen physiology and, subsequently, antibiotic resistance remain poorly understood. Here we demonstrate that physiologically-relevant reductions in pH increased *K. pneumoniae* beta-lactam resistance as much as 64-fold, with the most dramatic increase observed for beta-lactams that specifically inhibit cell division. We identified two genes that contribute to acid-dependent beta-lactam resistance, the class A PBP, PBP1b, and the paralogous class B PBP, $PBP3_{PARA}$. Loss of either PBP1b or $PBP3_{PARA}$ increases *K. pneumoniae* susceptibility to beta-lactams at low pH. Altogether these data emphasize the importance of functional redundancy among cell wall synthesis enzymes which allows for specialization and ensures robust cell wall synthesis across a range of environmental conditions.

Importance

Beta-lactams are the most prescribed class of antibiotics, but their effectiveness is threatened by a global rise in antimicrobial resistance. How the environment within a host or infection site shapes pathogen response to antibiotics is frequently overlooked in assessments of antibiotic effectiveness. We demonstrate that growth at physiologically-relevant low pH substantially increases *Klebsiella pneumoniae* resistance to clinically important beta-lactams. An important finding of this study is that during growth in acidic pH *K. pneumoniae* has a different repertoire of cell wall synthesis genes available than during growth at neutral pH due to the presence of acid-

29 inducible paralogous copies of essential cell wall synthesis enzymes, PBP2 and PBP3. An
30 additional functionally-redundant enzyme, PBP1b, also contributes to acid-dependent beta-
31 lactam resistance. Together, these findings expand our understanding of how bacteria maintain
32 cell wall synthesis across diverse physiochemical environments and highlight potential new
33 therapeutic targets.

34 **Introduction**

35 Infections caused by the ESKAPE pathogen *K. pneumoniae* are increasingly difficult to treat due to
36 dramatic rises in antibiotic resistance. *K. pneumoniae* is a dominant member of two different Beta-
37 lactam-resistant groups of bacteria, Extended-spectrum-Beta-lactamase (ESBL)-producing
38 *Enterobacteriaceae* and Carbapenem-resistant *Enterobacteriaceae* (CRE) which are labeled
39 serious and urgent public health threats by the CDC[1]. In 2019, *K. pneumoniae* was the third leading
40 cause of global deaths where the death was directly due to or associated with antibiotic
41 resistance[2]. While ESBLs and related enzymes are major contributors to beta-lactam resistance in
42 Gram-negative bacteria, data from our group and others identifies physicochemical parameters
43 consistent with a host environment are under-appreciated drivers of resistance. Changes in pH,
44 nutrient availability, and accumulation of the alarmone, ppGpp, increase antibiotic resistance
45 across a range of bacterial pathogens, highlighting the need to better understand how
46 environmental factors impact pathogen physiology[3–6].

47 Despite the prevalence of resistance markers such as ESBLs, beta-lactams remain the most
48 prescribed antibiotic class[7]. Beta-lactams interfere with the synthesis of the cell wall or
49 peptidoglycan (PG), an essential structure that provides shape and structural rigidity. PG is
50 comprised of glycan strands of repeating linked N-acetylglucosamine (NAG) and N-acetylmuramic
51 acid (NAM) sugars that are crosslinked together by short peptide chains [8]. Synthesis and
52 maintenance of PG requires many enzymatic steps that occur across multiple cellular locations;
53 PG precursors are built in the cytoplasm, transported through the inner membrane, and fully
54 assembled into PG within the periplasmic space. Amongst the *Enterobacteriaceae,* periplasmic PG
55 assembly is highly enzymatically redundant, with an average of four enzymes capable of carrying
56 out a single periplasmic PG synthesis reaction[9] . This apparent functional redundancy is
57 particularly striking when compared to the earlier cytoplasmic PG synthesis reactions, which occur
58 in a nearly 1:1 enzyme-to-reaction ratio[10]. While precursors are assembled in the relatively buffered

59 cytoplasm, the cell wall itself is built in the periplasm and thus exposed to the physicochemical
60 environment.

61 Penicillin-binding proteins (PBPs) carry out essential transpeptidation reactions in the periplasm.
62 Class A PBPs are bi-functional enzymes that both link the NAG-NAM sugar moieties together
63 (transglycosylation, TG) as well as crosslink the peptide stems of adjacent glycan strands
64 (transpeptidation, TP). In *Escherichia coli,* the primary class A PBPs are PBP1a and PBP1b, which
65 are encoded by *mrcA* and *mrcB* respectively. PBP1a and PBP1b are individually dispensable for
66 growth, but loss of both is lethal[11–13]. A third class A PBP, PBP1c (*pbpC*), has an unknown role in PG
67 synthesis and maintenance and is dispensable under standard laboratory conditions[14]. Class B
68 PBPs are monofunctional transpeptidases; these PBPs work in conjunction with cognate
69 glycosyltransferases. PBP2 and PBP3 are the canonical class B PBPs in Gram-negative bacteria,
70 and they function within the elongation and division machinery respectively.

71 Beta-lactams interfere with PG synthesis by irreversibly binding to the transpeptidase domain of
72 PBPs and inhibiting transpeptidation[7]. Our previous work indicates that growth in acidic pH (~pH 5)
73 substantially increases *E. coli* resistance to PBP2- and PBP3-targeting Beta-lactams. Both growth
74 in pH values < 5, as well as acid-dependent Beta-lactam resistance required the Class A PBP,
75 PBP1b, while full fitness during growth in alkaline pH required PBP1a[3]. To determine if this
76 response is conserved amongst other *Enterobacteriaceae*, we evaluated the impact of
77 environmental pH on *K. pneumoniae* resistance to beta-lactams.

78 Here we report that *K. pneumoniae* beta-lactam resistance increased as much as 64-fold during
79 growth in acidic conditions. Genetic analysis identified two cell wall synthesis genes, *mrcB* and
80 *ftsI2,* that are critical for pH-dependent changes in antibiotic resistance. *mrcB* encodes PBP1b, a
81 bifunctional class A PBP previously identified as a contributor to pH-dependent antibiotic
82 resistance in *E. coli*[3]. Induced at low pH, *ftsI2* encodes $PBP3_{PARA,}$ a paralogous copy of the
83 canonical, division-associated class B PBP, PBP3. $PBP3_{PARA}$ is required for both acid-dependent
84 beta-lactam resistance and robust growth and division at low pH. Altogether our findings highlight
85 that functional redundancy in bacterial PBPs confers fitness advantages and contributes to
86 environmentally-driven antibiotic resistance.

87 **Results**

88 ***Klebsiella pneumoniae* exhibits acid-dependent resistance to Beta-lactam antibiotics.**

89 To determine the impact of pH on *K. pneumoniae* beta-lactam susceptibility, we assessed the
90 response of a urinary tract infection (UTI) isolate, *K. pneumoniae* TOP52[15] to a panel of beta-
91 lactams during growth across a range of physiologically relevant pH conditions. The drug panel
92 included beta-lactams that preferentially target PBPs in the divisome (i.e. Cephalexin, Aztreonam,
93 and Piperacillin) or the elongasome (Meropenem, Doripenem), as well as non-specific inhibitors
94 (Ampicillin, Carbenicillin) that are reported to have similar affinities for all PBPs[16,17]. Relative
95 susceptibility or resistance to a given Beta-lactam was determined by comparing the minimal
96 inhibitory concentration of drug at neutral pH to that at other pH values.

97 *K. pneumoniae* exhibited a 2- to 64-fold increase in resistance to the entire spectrum of tested
98 beta-lactams when grown in LB at pH values < 5 relative to resistance at pH 7. (Fig 1A, Supp Table
99 4). We observed strong acid-dependent increases in resistance for drugs that preferentially target
100 PBP3, with Aztreonam (AZT) and Cephalexin (CEX) MICs increasing as much as 20- and 64-fold
101 respectively at pH 4.8. Resistance to PBP2-targeting Beta-lactams increased modestly at low pH,
102 with MICs to Doripenem (DOR) and Meropenem (MER) increasing 2- to 4-fold. In contrast to *E. coli*[3],
103 we also observed modest 2- to 4-fold increases in resistance to the non-specific Beta-lactams,
104 Ampicillin (AMP) and Carbenicillin (CAR) at low pH. At these pH values, increases in MICs during
105 growth at low pH are not due to significant antibiotic degradation[3].

106 Low pH not only enabled growth at concentrations of drug that are lethal at neutral pH but also
107 preserved cell morphology (Fig 1 C & D). Consistent with increased intrinsic resistance at low pH,
108 the characteristic rod-shaped morphology of *K. pneumoniae* was preserved during growth under
109 acidic conditions in concentrations of beta-lactams that cause either cell rounding (Meropenem)
110 or filamentation (Cephalexin) at neutral pH. The observed acid-dependent increased resistance to
111 beta-lactams is not strain specific behavior as *K. pneumoniae* strains NTUH-K2044 and ATCC
112 43816 also exhibit a 4-fold increase to Meropenem (MER) and an ~32-fold increase to Cephalexin
113 (CEX) when grown at pH 4.8 versus pH 6.8 (Fig. 1B).

114 To determine if this behavior also occurs under conditions that better reflect a native host
115 environment, we assayed how *K. pneumoniae* responded to beta-lactams during growth in an
116 artificial urine growth medium at low and neutral pH[18]. Similar to growth in LB, we observed 32- to
117 >64-fold increases in resistance to Ampicillin and Cephalexin in acidified artificial urine with and
118 without amino acid supplementation compared to neutral pH (Sfig 1, Supp table 4 & 5). While the
119 MIC for a given beta-lactam was generally higher during growth at low pH independent of media

120 composition, we observed that for certain antibiotics the media composition coupled with
121 acidification of the media significantly altered the susceptibility. The MIC for Ampicillin at low pH in
122 LB was significantly lower (mean MIC = 104 ug/mL ± 37) than during growth in AU (mean MIC =
123 2500 ug/mL ±0.0), indicating an interplay between nutrient composition and pH. We were unable to
124 determine the exact foldchange in MIC for Cephalexin, as *K. pneumoniae* grew in all tested
125 concentrations of Cephalexin in both AU and AU+AA (Sfig 1, table 4 & 5). Together our data suggest
126 that acid-dependent beta-lactam resistance occurs across a range of nutrient conditions and is
127 conserved amongst *K. pneumoniae* lineages.

128 **Acid-dependent Beta-lactam resistance is independent of endogenous beta-lactamase**
129 **expression.**

130 *K. pneumoniae* TOP52 encodes an endogenous class-A beta-lactamase, bla_{SHV-1}, which confers
131 increased resistance to the Penicillin subclass of Beta-lactams[7,15,19]. To determine if expression of
132 bla_{SHV-1} is influencing the resistance profiles at low pH, we generated a deletion strain (Δbla_{SHV-1})
133 and repeated the MIC assays under both acidic and neutral pH conditions. We observed increased
134 sensitivity to the Penicillin sub-classes of Beta-lactams tested (AMP, CAR, PIP) in both pH
135 environments (Sup Table 5). Consistent with the specificity of bla_{SHV-1}, loss of bla_{SHV-1} did not alter
136 the MICs to non-Penicillin beta-lactams at either pH (Sup Table 5). However, the Δbla_{SHV-1} mutant
137 still displayed increased resistance to all tested Beta-lactams at low pH relative to neutral pH (Fig 2
138 A-D, Supp table 5), demonstrating that acid-dependent resistance is independent of endogenous
139 beta-lactamase expression.

140 **pH modulates expression of Class B PBP paralogs in *K. pneumoniae*.**

141 To ascertain the impact of pH on expression of genes encoding PBPs or other cell wall synthesis
142 genes, we performed RNAseq in *K. pneumoniae* comparing cells cultured in pH 4.8 LB versus pH
143 6.8 LB (Supp table 7). Consistent with previous studies, pH does not impact expression of class A
144 PBPs, *mrcA* (PBP1a) or *mrcB* (PBP1b), in either *E. coli* or *K. pneumoniae*[20,21] (Table 1). Class A PBP
145 activity is regulated by cognate outer membrane activators, LpoA and LpoB[22–24] . We observed that
146 the PBP1b activator, encoded by *lpoB,* was down-regulated ~2-fold at low pH.PBP1c, a cryptic
147 class A PBP with no demonstrated role in cell wall synthesis under standard laboratory conditions,
148 exhibited an ~2-fold decrease in expression during growth in acidic pH (Table 1, Supp table 7). We
149 observed no significant changes expression of the class B PBPs between pH conditions, but there

150 was an order of magnitude increase in expression at low pH of genes we designated *mrdA2* and
151 *ftsI2*, which encode paralogous copies of class B PBPs, referred to here as $PBP2_{PARA}$ and $PBP3_{PARA}$
152 (Fig 3 A&B). In addition to the class B paralogs, several other cell wall synthesis genes displayed
153 pH-responsive expression profiles. Most notably, two carboxypeptidases, *dacA* (PBP5) and *dacD*
154 (PBP6b), exhibited modest increases of 2- to 3-fold in expression during growth at low pH. Both
155 *dacA* and *dacD* are implicated in maintaining proper cell morphology in *E. coli*, with *dacD* being
156 required for proper morphology specifically at low pH[25,26].

157 **Loss of $PBP3_{PARA}$ results in filamentation in *K. pneumoniae* at low pH.**

158 Duplications of the class B PBPs, PBP2 and PBP3, that have expanded the repertoire of cell wall
159 synthesis enzymes have been described in several pathogens[27–29]. Class B PBP paralogs in
160 *Salmonella enterica* serovar Typhimurium (*S.* Typhimurium) referred to as $PBP2_{SAL}$ and $PBP3_{SAL}$ are
161 thought to be important for maximal fitness during growth at low pH. Expression of both $PBP2_{SAL}$
162 and $PBP3_{SAL}$ is maximally induced at low pH (<5.8), and loss of $PBP2_{SAL}$ has been reported to impair
163 rod-shape morphology under acidic environments[28,29].

164 As with $PBP2_{SAL}$ and $PBP3_{SAL}$, $PBP2_{PARA}$ and $PBP3_{PARA}$ share significant sequence identity with their
165 canonical counterparts (59% for $PBP2_{PARA}$ and 61% for $PBP3_{PARA}$) and retain the sequence motifs
166 associated with catalysis, but their contributions to cell wall maintenance in *Klebsiella* are
167 unknown (Fig 3 C&D, Sfig 2). We generated individual gene deletion strains and examined the
168 mutants using cell size analysis and time-lapse microscopy to evaluate the role of the class B PBP
169 paralogs in cell size and division. We cultured cells at both acidic and neutral pH and sampled
170 cultures at early exponential phase (OD_{600} = 0.1-0.2) for cell size analysis. While loss of $PBP2_{PARA}$ did
171 not impact cell size or morphology at either pH, we found that during growth at pH 4.8 the $PBP3_{PARA}$
172 deletion mutant exhibited heterogeneous cell lengths, with many cells displaying filamentous
173 behavior indicative of cell division defects (Fig4 A&B, Sfig 3). Using a definition of filamentation as a
174 cell length of >15 μM which represents ~3X the average length of WT cells at pH 4.8 (3.9 ± 0.2 μM,
175 Fig 4B), we determined that 21-58% of $PBP3_{PARA}$ deficient cells within a given population were
176 filamentous, with a smaller proportion of cells (3-17%) reaching lengths of >40 μM. The division
177 defects associated with loss of $PBP3_{PARA}$ were specific to growth in acidic conditions, as growth at
178 neutral pH resulted in an average cell length for the $PBP3_{PARA}$ deficient cells consistent with WT cell
179 lengths (Fig 3C).

180 Time-lapse microscopy of acid-grown Δ*ftsI2* cells spotted onto acidic LB agarose pads revealed a
181 population of cells with heterogeneous lengths that displayed clear division defects as cells
182 continued to elongate without successful division resulting in long filamentous cells. Whereas
183 spotting acid-grown Δ*ftsI2* cells onto LB agarose pads at neutral pH restored division to the
184 filamentous cells (Sfig 4). Complementation of *ftsI2* in trans from a medium-copy number plasmid
185 enabled division and restored cell lengths consistent with WT at low pH (Fig 4 A&B). Together these
186 data suggest that the activity of the canonical PBP3 is impaired under acidic conditions and that
187 $PBP3_{PARA}$ is the predominant transpeptidase supporting cell division in *K. pneumoniae* at low pH.

188 **Loss of PBP1b or $PBP3_{PARA}$ differentially impacts Beta-lactam resistance at low pH in *Klebsiella***

189 The increased expression of genes encoding $PBP2_{PARA}$ and $PBP3_{PARA}$ and other cell wall
190 maintenance proteins at low pH raised the possibility that these proteins might contribute to acid-
191 dependent Beta-lactam resistance. To address this hypothesis, we generated strains individually
192 defective in a subset of *K. pneumoniae* genes implicated in cell wall or shape maintenance and
193 assayed their response to beta-lactam antibiotics during growth at acidic and neutral pH
194 conditions. In addition to genes that displayed pH-dependent expression, we also evaluated the
195 role of class A PBPs in *K. pneumoniae* response to beta-lactams across pH conditions, as these are
196 known to influence antibiotic response in *E. coli*. While most individual mutations did not
197 significantly impact acid-dependent-Beta-lactam resistance, loss of PBP1b or $PBP3_{PARA}$ altered
198 sensitivity to Beta-lactams at low pH (Fig 2A-D, Supp table 6).

199 Loss of PBP1b (Δ*mrcB*) most dramatically affected acid-dependent resistance to Cephalexin. A
200 Δ*mrcB* mutant displayed only a 4-fold increase in cephalexin MIC at low pH versus at neutral pH,
201 while the WT has a 64- to 128-fold increase in resistance under the same conditions. The Δ*mrcB*
202 mutant also no longer exhibited acid-dependent resistance to the generalist (AMP) and PBP2-
203 targeting- (DOR, MER) beta-lactams, (Fig 2 A-D, Sfig 6, Supp table 6).The increased beta-lactam
204 sensitivity of a PBP1b deletion mutant at low pH is likely due to loss of the enzyme activity under
205 this condition. Deletion of PBP1b's cognate outer membrane activator lpoB (Δ*lpoB*) results in
206 similar sensitization levels at low pH as a PBP1b mutant (Sfig 6, Supp Table 6). Defects in PBP1b
207 also led to a nearly 10-fold increase in susceptibility to Cefsulodin in both acidic and neutral pH
208 compared to WT (Sup Table 6). This pH-independent increase in sensitivity of the ΔPBP1b mutant
209 is consistent with data suggesting that PBP1a is the primary Class A target of Cefsulodin[30,31].

210 Loss of $PBP3_{PARA}$ differentially impacted resistance to beta-lactams. The $PBP3_{PARA}$ null mutant no
211 longer displayed acid-dependent resistance to Ampicillin and Cefsulodin at low pH (Fig 2A & B). In
212 fact, a $PBP3_{PARA}$ deletion mutant was more sensitive to Ampicillin at low pH than at neutral pH (Fig
213 2A). When challenged with PBP3-targeting Beta-lactams (CEX, AZT, PIP), the $PBP3_{PARA}$ deletion
214 mutant still retained mild acid-dependent resistance but was 2- to 8-fold more sensitive at low pH
215 than WT (Fig 4 D, 5 B). Surprisingly, the $PBP3_{PARA}$ null mutant exhibited increased resistance when
216 challenged with PBP2-targeting beta-lactams at low pH. The Meropenem and Doripenem MICs
217 obtained for the $PBP3_{PARA}$ null mutant were 12-16-fold higher at acidic pH versus neutral pH. For
218 comparison, WT cells only exhibited a 2-4-fold increase in MIC to these two drugs at acidic pH (Fig
219 4C, 5A). Despite the ~10-fold increases in expression under acidic conditions, loss of *mrdA2,*
220 encoding PBP2, had no significant impact on Beta-lactam susceptibility across pH values.

221 **Increased acid-dependent resistance to PBP2-targeting compounds in the $PBP3_{PARA}$ null**
222 **mutant requires $PBP2_{PARA}$.**

223 We reasoned that the unexpected increase to PBP2-inhibitors at low pH observed in the Δ*ftsI2*
224 mutant could be influenced by the presence of $PBP2_{PARA}$. To address this possibility, we generated
225 a double deletion strain lacking both class B paralogs (Δ*ftsI2* Δ*mrdA2*) and assayed its response to
226 beta-lactams with high specificity for PBP2 or PBP3 at both neutral and acidic pH. Deletion of both
227 class B PBP paralogs eliminated the dramatic increase in resistance at low pH (4.8), restoring WT-
228 level responses to both Doripenem and Meropenem. When challenged with PBP3-targeting Beta-
229 lactams, the double mutant class B paralog mutant phenocopied the Δ*ftsI2* mutant, displaying
230 similar reductions in resistance at low pH (Fig 5). Together these data suggest that both $PBP2_{PARA}$
231 and $PBP3_{PARA}$ are involved in mediating resistance to PBP2-inhibitors, whereas resistance to PBP3-
232 targeting Beta-lactams is primarily facilitated by $PBP3_{PARA}$.

233 **Discussion**

234 As observed in *E. coli,* beta-lactam resistance in *K. pneumoniae* increases substantially during
235 growth in acidified medium (Fig 1A). Importantly, we observed pH-dependent increases in beta-
236 lactam resistance in LB as well as in a more physiologically relevant medium, artificial urine (Fig 1,
237 Sfig 1). We find that the class A PBP, PBP1b, and the acid-responsive paralogous copy of the class
238 B PBP, $PBP3_{PARA}$, are major genetic contributors to acid-mediated beta-lactam resistance in *K.*
239 *pneumoniae*. Disruption of *mrcB*, the gene encoding PBP1b, eliminates acid-mediated resistance

240 to the class B PBP inhibitors, Meropenem, Doripenem, and Cephalexin. Loss of $PBP3_{PARA}$
241 differentially impacts beta-lactam resistance, with mutants showing sensitization towards
242 Ampicillin, Cefsulodin, and all PBP3-targeting beta-lactams but increased resistance towards
243 PBP2-targeting antibiotics.

244 While both *E. coli* and *K. pneumoniae* demonstrate acid-dependent beta-lactam resistance,
245 factors influencing this phenomenon differ between the two organisms. Acid-mediated beta-
246 lactam resistance in *E. coli* appears to be solely due to intrinsic properties of the PBP enzymes,
247 particularly PBP1b[3], while in *K. pneumoniae* the contribution of PBP1b is supplemented by pH-
248 dependent induction of genes encoding paralogous class B PBPs. Although we only observed
249 strong changes to antibiotic susceptibility in a $PBP3_{PARA}$ null mutant, loss of $PBP2_{PARA}$ impacted the
250 resistance to PBP2-targeting antibiotics in a $PBP3_{para}$ null background, as well as the morphological
251 response at low pH (Fig 5 C). This result suggests that $PBP2_{PARA}$ plays a role in maintaining PG and
252 cell shape at low pH. Together, our findings support a modular model of cell wall synthesis within
253 the *Enterobacteriaceae* family where apparent function redundancy amongst cell wall synthesis
254 enzymes is protective by enabling PG synthesis across a range of pH conditions.

255 **The Class A PBP, PBP1b, is important for acid-dependent beta-lactam resistance in *K.***
256 ***pneumoniae***

257 PBP1b is required for resistance to PBP2- and PBP3-targeting beta-lactams and for growth at low
258 pH (<5) in *E. coli*[3]. In contrast, deletion of PBP1b in *K. pneumoniae* did not significantly impair
259 growth in acidified culture medium (pH 4.8), suggesting that there are key differences in how PBP1b
260 influences growth in acidic environments between *E. coli* and *K. pneumoniae* (Sfig 5). While
261 expression of *mrcB,* encoding PBP1b, was not influenced by pH, loss of PBP1b impaired *K.*
262 *pneumoniae's* resistance to Ampicillin, Doripenem, Meropenem, and Cephalexin at low pH (Fig 2,
263 Supp Table 5). Consistent with MIC data, a PBP1b-deficient strain exhibits faster killing kinetics
264 than a WT strain in the presence of Cephalexin at low pH (Fig 2 E &F). While filamentation is a
265 characteristic morphology associated with division-targeting beta-lactams[32,33], at low pH a PBP1b-
266 deficient *K. pneumoniae* strain is sensitive to Cephalexin at concentrations that do not elicit
267 filamentation (Fig 4E). The time frame for lysis of the PBP1b mutant is rapid with more than 50% of
268 the population exhibiting lysis or loss of membrane integrity as denoted by propidium iodide
269 staining within 90 minutes of exposure to Cephalexin at low pH (Fig 2F).

270 Notably, at neutral pH loss of PBP1b or its cognate outer membrane activator, LpoB, mutant did not
271 significantly alter MICs across beta-lactam classes (Sup Table 5), suggesting that PBP1B specifically
272 mediates beta-lactam resistance at low pH in *K. pneumoniae*. This finding differs from what has
273 been observed in *E. coli* where loss of either PBP1b or LpoB increases sensitivity to multiple classes
274 of beta-lactams at neutral pH[34,35]. This result is also consistent with prior data suggesting that PBP1a
275 does not function optimally under acidic conditions and therefore cannot compensate for loss of
276 PBP1b activity at low pH[3]. Our data demonstrating that a PBP1b mutant is more sensitive to PBP2-
277 and PBP3-targeting beta-lactams is consistent with prior studies reporting interactions between
278 PBP1b and key division and elongasome proteins[36,37,29]. Based on these data, we propose that PBP1b
279 supports cell wall integrity at low pH through interactions supporting other cell division proteins.

280 **Class B PBP paralogs differentially modulate pH-dependent changes in beta-lactam**
281 **resistance**

282 Although, low pH induced expression of genes encoding both *K. pneumoniae's* PBP2 and PBP3
283 paralogs (Table 1), only loss of *ftsI2,* encoding $PBP3_{PARA}$, sensitized cells to beta-lactams during
284 growth in acidified medium. These data are consistent with observations in *S.* Typhimurium that
285 loss of its PBP3 paralog, $PBP3_{SAL}$sensitizes cells to beta-lactams targeting division[38].Defects in
286 *mrdA2*, encoding $PBP2_{PARA}$, did not significantly impact beta-lactam resistance at either acidic or
287 neutral pH. In *K. pneumoniae* loss of $PBP3_{PARA}$ at low pH sensitized cells to not only PBP3 inhibitors,
288 but also to a Cephalosporin targeting class A PBPs and the penicillin, Ampicillin (Figure 4 A&B).
289 While loss of $PBP3_{PARA}$ generally sensitized *K. pneumoniae* to beta-lactams under acidic conditions,
290 it increased resistance to compounds targeting PBP2 at pH 4.8 up to 12- to 16-fold (Figure 5A). This
291 increase in resistance in $PBP3_{PARA}$ deficient cells was eliminated in a double mutant lacking both
292 $PBP3_{PARA}$ and $PBP2_{PARA}$ (Δ*ftsI2* Δ*mrdA2*). Under acidic conditions the double class B paralog mutant
293 exhibited WT-level MICs when challenged with Meropenem or Doripenem (Figure 5).

294 It is unclear why the loss of $PBP3_{PARA}$ renders cells resistant to PBP2-targeting compounds.
295 Morphological data of WT *K. pneumoniae* challenged with Meropenem at low pH reveals hybrid
296 morphologies, with cells displaying signatures of both divisome and elongasome inhibition. Cells
297 first undergo lengthening and then display large, rounded septal bulges (Fig 5C). These results
298 could reflect altered target binding by Meropenem at low pH, where PBP3/$PBP3_{PARA}$ are also
299 inhibited along with PBP2/$PBP2_{PARA}$. Alternatively, physical interactions between class B PBPs
300 within the elongasome and divisome have been reported in *E. coli*[39], and data suggests that the

301 protein components of the PG synthesis complexes in *Salmonella* vary depending on whether the
302 canonical or paralogous class B PBP is present in the complex[29,40]. Alterations to interactions
303 between class B PBP paralogs and other cell wall synthesis proteins due to beta-lactam binding or
304 in the class B PBP paralog mutant backgrounds could influence morphology and antibiotic
305 resistance. Additional work is needed to fully understand the complex role that the class B PBP
306 paralogs play in resistance to PBP2-targeting beta-lactams.

307 **$PBP3_{PARA}$ is critical for *K. pneumoniae* division at low pH**

308 Our data suggest that $PBP3_{PARA}$ is the major transpeptidase supporting cross wall synthesis at low
309 pH. Loss of $PBP3_{PARA}$ did not impact cell length at neutral pH but impaired division at low pH,
310 resulting in filamentous cells. However, these acid-cultured $PBP3_{PARA}$-deficient filamentous cells
311 were able to resume division and return to WT-lengths if they were transitioned to neutral pH
312 (Sfig3), suggesting that the canonical PBP3 is unable to fully compensate for the loss of $PBP3_{PARA}$ at
313 low pH. We attempted to disrupt the canonical PBP3 under acidic culture conditions where
314 $PBP3_{PARA}$ is likely the dominate division-specific transpeptidase; however, despite multiple
315 attempts, we were unsuccessful. Moreover, a small percentage of Δ*ftsI2* cells maintained WT-
316 lengths at low pH, suggesting that the canonical PBP3 retains limited, but critical activity at low pH
317 (Sfig 3). These data differ from *Salmonella* where the canonical PBP3 and PBP3 paralog $PBP3_{SAL}$ are
318 individually dispensable at low pH. The canonical PBP3 is capable of supporting growth at both low
319 and neutral pH, but $PBP3_{SAL}$ is unable to support division at neutral pH[28]. Our results support a
320 model in which *K. pneumoniae* PBP3 functions optimally at neutral pH while $PBP3_{PARA}$ functions
321 predominately at acidic pH, with both working together to ensure that division remains robust
322 across pH conditions.

323 **Expansion and pH specialization of *K. pneumoniae* cell wall synthesis enzymes provide novel**
324 **therapeutic targets**

325 Identification of paralogous class B PBPs has thus far only been described in pathogens [27–29,41], but
326 the role of these paralogous cell wall synthesis proteins in pathogen physiology remains largely
327 uncharacterized. In *Salmonella,* the acid-responsiveness of class B PBP paralogs raised
328 speculation that they could be critical to support bacterial survival during intracellular growth
329 within acidified host immune cells. However, loss of the class B PBP paralogs did not impair
330 replication within macrophages or attenuate virulence in a mouse infection model[28].

331 In *Klebsiella pneumoniae,* our data suggests that class B PBP paralogs are part of a general strategy
332 of functional redundancy to preserve critical enzymatic activity across a wide range of
333 environmental conditions. Colonization of a host exposes a bacterial pathogen to a wide range of
334 pH conditions[42–44] . We demonstrate that the acidification of growth medium to physiologically-
335 relevant levels is sufficient to increase resistance to beta-lactams. The class B PBP paralogs
336 modulate that resistance in part, suggesting that these pathogen-specific proteins may provide
337 novel therapeutic targets. We propose that future screens for new antimicrobial targets factor
338 environmental pH as a variable to identify novel compounds that can bind to acid-responsive
339 targets such as the Class B PBP paralogs. Altogether, our results highlight the need to evaluate
340 pathogen physiology in diverse environments beyond the standard laboratory conditions.

341 **Acknowledgements**

342 We thank members of the Levin lab for their feedback and discussion regarding this study, with a
343 special thanks to Kyra Raines and Dr. Sarah Anderson for critical reading of this manuscript. We are
344 also grateful to David Rosen and his group for the gift of TOP52 and welcome advice on genetic
345 manipulation of *K. pneumoniae*. This work has been funded by the NIH through an R35-GM127331
346 award to P.A.L.

347 **Contributions**

348 S.B.: Conceptualization, Investigation, Formal analysis, Methodology, Visualization, Writing-
349 original draft, Writing – review and editing.

350 P.A.L.: Conceptualization, Funding acquisition, Resources, Supervision, Writing – review and
351 editing.

352 **Data availability**

353 All raw and processed data required to evaluate the conclusions of this study are included in the
354 text or supplemental data. The RNA sequencing data for gene expression studies at acidic and
355 neutral pH have been deposited in the NCBI GEO repository: GSE291667.

356 **Methods**

357 **Bacterial strains, growth conditions, and antibiotics.**

358 Bacterial strains and plasmids used in this study are listed in Supplementary table 1 and
359 Supplementary table 2. Strains were routinely cultured in Lysogeny Broth (LB – 1% Tryptone, 0.5%
360 Yeast extract, and 1% NaCl) in large glass tubes at 37 °C with 200 RPM aeration. The pH of LB was
361 adjusted with 1:10 MMT buffer (1:2:2 molar ratio of D/L-malic acid, MES, and Tris base). Artificial
362 urine (AU) was prepared as described[18], and cells were cultured in either base AU or AU
363 supplemented with all twenty amino acids at a final concentration consistent with what is used in
364 EZ rich defined medium (https:www.genome.wisc.edu/resources/protocols/ezmedium.htm). The
365 pH of AU or AU+AA was adjusted with MMT buffer immediately prior to use. For ease and clarity,
366 media and amino acid composition is listed in Supp table 8.

367 Where indicated cultures were supplemented with Kanamycin (50 µg/mL), Spectinomycin (100
368 µg/mL), Chloramphenicol (50 µg/mL), or IPTG (0.1 mM) . The pRDC3 plasmid (p15A ori, SpecR,
369 Plac) was a gift from Fabrizio Arigoni. Plasmid pSDB8 was generated from pRDC3 using the IVA
370 cloning method to insert *ftsI2* under control of the Plac promoter[45]. Primers were acquired from
371 Integrated DNA Technologies (Coralville, IA) and sequences used are listed in Supp Table 3.
372 Chemically competent *E. coli* TOP10 (Invitrogen) were used to assemble vectors via IVA. Plasmid
373 sequence was confirmed via whole plasmid sequencing at Plasmidsaurus prior to transformation
374 into *K. pneumoniae* strains.

375 For growth studies, cultures were started in LB supplemented with MMT buffer to the indicated pH
376 and grown in large glass tubes at 37 °C with 200 RPM aeration. Cultures were harvested once they
377 reached mid-exponential phase (OD_{600} =0.2-0.6), concentrated to an OD_{600} =1.0, and serially
378 diluted 10-fold. 1.5 µL of the 10^{-5} dilution was used to inoculate wells of sterile 96-well plates
379 containing 150 µL of LB + MMT at indicated pH. The plate was covered with a Breathe-Easy strip
380 (Diversified Biosciences) and growth was monitored in a BioTek Synergy H1 plate reader with the
381 following settings: 37 °C, continuous double orbital shaking at 282 cpm, with OD_{600} readings taken
382 every 10 minutes.

383 For *ftsI2* cell size complementation studies, un-induced overnight cultures of strains carrying either
384 pRDC3 (Empty vector, EV) or pSDB8 were back-diluted 1:500 into 3 mL of fresh LB buffered to
385 either pH 4.8 or pH 6.8 containing Spectinomycin (100 µg/mL). Cultures were grown at 37 °C with
386 200 RPM aeration for 1.5 hrs. Expression of *ftsI2* was induced with the addition of 0.1 mM IPTG and
387 cultures were allowed to continue growing until early exponential phase (OD_{600} = 0.1-0.3) was
388 reached (~40-90 additional minutes). Cultures were back-diluted into fresh buffered media

389 containing Spectinomycin (100 µg/mL) and 0.1 mM IPTG to an OD_{600} ~= 0.005. Growth was
390 monitored every 30 minutes, and cells were harvested when cultures reached early exponential
391 phase (OD_{600} = 0.1-0.3). Cells were spotted onto media pads (LB + MMT (pH 4.8 or 6.8) +
392 Spectinomycin (100 µg/mL) + 0.1 mM IPTG + 1% agarose) and imaged live with phase microscopy.

393 The following antibiotics were used for antibiotic susceptibility screenings. Ampicillin sodium salt,
394 Aztreonam, Cephalexin hydrate, Cefsulodin sodium salt hydrate, Meropenem Trihydrate, and
395 Piperacillin sodium salt were obtained from Sigma Adrich (St. Louis, MO). Carbenicillin sodium salt
396 was from EMD Millipore (now Millipore Sigma, Germany). Doripenem was obtained from Cayman
397 Chemicals (Ann Arbor, MI).

398 **Genetic manipulation:** Gene disruptions were carried out in the *K. pneumoniae* TOP52
399 background using a Lambda Red vector modified to carry a Spectinomycin resistance cassette as
400 described previously [46,47]. Briefly, DreamTaq Polymerase (Thermo Scientific) was used to PCR
401 amplify the Kanamycin resistance cassette from the template plasmid pKD4 with primers
402 containing 40-60 bp of homology to the chromosomal targets. Primers were designed to leave the
403 start and stop codons of the targeted gene intact. In cases where the two gene sequences
404 overlapped, primers were designed to avoid disruption to any downstream genes. Linear PCR
405 products were purified using a Purelink PCR purification kit (Invitrogen), and 2,000-3,000 ng of
406 purified linear fragments were electroporated into *K. pneumoniae* cells grown in the presence of
407 0.7% L-arabinose to induce expression of the Lambda Red recombinase system from the pKD46S
408 plasmid. Electroporated cells were recovered in SOC (Lloyd's recipe – 2% Tryptone, 0.5% yeast
409 extract, 10 mM NaCl, 2.5 mM KCl, 10 mM $MgSO_4$, 20 mM glucose) for 4-8hrs at 30°C. Deletion
410 mutants were selected for by plating transformation culture onto LB agar plates containing
411 Kanamycin (50 µg/mL) and incubated at 37°C. Mutants were confirmed by colony PCR and
412 sequencing as necessary. For marker-less deletions, cells were transformed with pCP20 at 30°C in
413 LB + Chloramphenicol (50 µg/mL) to express the FLP to excise the FRT-flanked Kanamycin
414 cassette. After excision, cells were cultured at 42°C to promote loss of pCP20. Kanamycin and
415 Chloramphenicol sensitivity was confirmed for strains prior to use.

416 **RNA sequencing**: *K. pneumoniae* TOP52 or *E. coli* MG1655 was cultured overnight in LB buffered
417 to either pH 4.8 or 6.8 with MMT buffer. Overnight cultures were back diluted 1:100 into fresh media
418 and cultured at 37°C with 200 RPM aeration until cultures reached early exponential phase (OD_{600}
419 =~0.2). ~ 9.6 x 10^8 cells were transferred to 15 mL conical Falcon tubes and pelleted by

420 centrifugation at 4°C (4,000 RPM for 10 mins). The supernatant was discarded, cell pellets were
421 resuspended in 350 uL of RNAwiz, and the RNA was extracted following the protocol for the
422 Ribopure-Bacteria RNA extraction kit [Invitrogen]. RNA was eluted in 50 uL of elution solution.
423 Purified RNA was subjected to a DNase I treatment to remove any contaminating chromosomal
424 DNA. RNA sequencing and differential gene expression analysis was performed by MiGS (now
425 SeqCenter). Quality control and adapter trimming of reads was performed with bcl2fastq. Read
426 mapping was performed with HISAT2, and read quantification was performed using Subread's
427 featureCounts. Read counts were normalized in R using edgeR's Trimmed Mean of M values (TMM)
428 algorithm, and subsequent values were converted to counts per million (CPM). Differential
429 expression analysis was performed using edgeR's Quasi-Linear F-Test (qlfTest) functionality
430 against treatment groups, and DEGs were considered as those with $|logFC| > 1$ and $p < .05$. Three
431 biological replicates were submitted per pH condition.

432 **Antibiotic susceptibility testing.** Cells were cultured from a single colony in LB at the indicated
433 pH to exponential phase (OD_{600} =~0.2-0.6) at 37 °C with 200 RPM aeration. For MICs in AU or
434 AU+AA, overnight cultures were back-diluted 1:100 into fresh media and cultured at 37 °C with 200
435 RPM aeration at the indicated pH to exponential phase (OD_{600} =~0.2-0.6). Harvested cells were
436 concentrated to an OD_{600} =1 and serially diluted 10-fold. 1.5 µL of the 10^{-2} dilution was used to seed
437 wells containing 150 µL of LB broth + MMT (matching pH) in sterile 96-well microtiter plates
438 containing a range of two-fold dilutions of beta-lactam antibiotics. Plates were sealed with a
439 Breathe-Easy strip (Diversified Biotech) and incubated for 20 hours at 37°C with 200 RPM aeration.
440 The minimal inhibitory concentration (MIC) was determined by visual inspection and reflects the
441 lowest drug concentration that completely inhibited bacterial growth.

442 **Terminal morphology Assessment.** At the end of 20 hours for antibiotic susceptibility tests, cells
443 were taken from wells following growth at either neutral or acidic pH with the indicated antibiotic
444 concentrations. 5 µL of cells were spotted onto LB + 1% agarose and imaged by phase contrast
445 microscopy.

446 **Microscopy, cell size analysis, and time-lapse Imaging.** All phase contrast and fluorescence
447 images were acquired on either a Nikon Ti-E inverted microscope or a Ti2-E inverted microscope
448 (Nikon Instruments). The Ti-E is equipped with a 100X Plan Apo oil objective (N.A. = 1.45 Ph3
449 objective, X-Cite 120 LED light source (Lumen Dynamics) and an OrcaERG CCD camera
450 (Hammamatsu Photonics, Bridgewater, N.J.) Filter cubes were purchased from Chroma

451 Technology Corporation. The Ti2-E inverted microscope is equipped with a 100X Plan Apo oil
452 objective (N.A. = 1.45, Ph3 objective, Lumencor Sola LED light engine (Lumencore), and an orca-
453 Fusion sCMOS camera (Hammamatsu Photonics). Filter cubes were purchased from Chroma
454 Technology Corporation. Both microscopes have an enclosed temperature-controlled enclosure to
455 pre-heat the objective to 37 °C (OXO enclosure) prior to experiments. Nikon Elements software was
456 used for image capture, and analysis was performed using the MicrobeJ plug-in in ImageJ.

457 For cell size analysis, cells were grown from a single colony in LB with MMT buffer at indicated pH
458 at 37 °C and 200 RPM aeration to exponential phase (OD_{600} = 0.2-0.4) and back-diluted to an OD_{600}
459 = 0.005 into 7 mL of pre-warmed LB + MTT (same pH). Growth was monitored via optical density,
460 and when cultures reached early exponential phase (OD_{600} =0.1- 0.2) cells were harvested. 5 µL of
461 cells were spotted onto LB + MTT (same pH)+ 1% agarose pads and imaged by phase contrast
462 microscopy. Cell morphology and size dimensions were determined using the MicrobeJ[48] plug-in
463 for ImageJ.

464 For time-lapse imaging, cultures were grown from a single colony in LB with MMT buffer at
465 indicated pH at 37 °C and 200 RPM aeration to exponential phase (OD_{600} = 0.1-0.4). 5 µL of cells
466 were spotted onto LB + MTT (same pH)+ 1% agarose pads that contain antibiotics at indicated
467 concentrations and 1.5 µM propidium iodide (PI) for monitoring loss of membrane integrity. Phase
468 images were obtained every 2 minutes, and fluorescent images were collected every 10 minutes
469 (Chroma AT560/40X/ Chroma AT600 DC/ Chroma at635/60nm with 100 mS exposure/10%
470 intensity). For each experiment a total of 2-5 different XY coordinates were monitored throughout
471 the duration of the experiment. Quantification of PI^+ cells was done using the MicrobeJ[48] plug-in for
472 ImageJ. Briefly the number of cells in the phase image and the number of corresponding
473 fluorescent cells were quantified. Data was reported as either percentage of PI^+ cells (number of PI^+
474 cells/total number of cells *100) or percent alive (number of cells-PI^+ cells/total number of
475 cells*100).

476 **Bibliography**

477 1. Centers for Disease Control and Prevention (U.S.). *Antibiotic Resistance Threats in the United*
478 *States, 2019*. https://stacks.cdc.gov/view/cdc/82532 (2019) doi:10.15620/cdc:82532.

2. Murray, C. J. *et al.* Global burden of bacterial antimicrobial resistance in 2019: a systematic analysis. *The Lancet* **399**, 629–655 (2022).
3. Mueller, E. A., Egan, A. J. F., Breukink, E., Vollmer, W. & Levin, P. A. Plasticity of Escherichia coli cell wall metabolism promotes fitness and antibiotic resistance across environmental conditions. *eLife* **8**, (2019).
4. Vinella, D., Albrecht, C., Cashel, M. & D'Ari, R. Iron limitation induces SpoT-dependent accumulation of ppGpp in Escherichia coli. *Mol Microbiol* **56**, 958–970 (2005).
5. Fanous, J. *et al.* Limited impact of Salmonella stress and persisters on antibiotic clearance. *Nature* **639**, 181–189 (2025).
6. Honsa, E. S. *et al.* RelA Mutant Enterococcus faecium with Multiantibiotic Tolerance Arising in an Immunocompromised Host. *mBio* **8**, (2017).
7. Bush, K. & Bradford, P. A. β-Lactams and β-Lactamase Inhibitors: An Overview. *Cold Spring Harbor Perspectives in Medicine* **6**, a025247 (2016).
8. Egan, A. J. F., Errington, J. & Vollmer, W. Regulation of peptidoglycan synthesis and remodelling. *Nature Reviews Microbiology 2020 18:8* **18**, 446–460 (2020).
9. Mueller, E. A. & Levin, P. A. Bacterial cell wall quality control during environmental stress. *mBio* **11**, 1–15 (2020).
10. Pazos, M., Peters, K. & Vollmer, W. Robust peptidoglycan growth by dynamic and variable multi-protein complexes. *Current Opinion in Microbiology* **36**, 55–61 (2017).
11. Kato, J., Suzuki, H. & Hirota, Y. Dispensability of either penicillin-binding protein -1a or -1b involved in the essential process for cell elongation in Escherichia coli. *Molec. Gen. Genet.* **200**, 272–277 (1985).

501 12. Suzuki, H., Nishimura, Y. & Hirota, Y. On the process of cellular division in Escherichia coli: a
502 series of mutants of E. coli altered in the penicillin-binding proteins. *Proceedings of the*
503 *National Academy of Sciences* **75**, 664–668 (1978).
504 13. Yousif, S. Y., Broome-Smith, J. K. & Spratt, B. G. Lysis of Escherichia coli by beta-lactam
505 antibiotics: deletion analysis of the role of penicillin-binding proteins 1A and 1B. *J Gen*
506 *Microbiol* **131**, 2839–2845 (1985).
507 14. Schiffer, G. & Höltje, J.-V. Cloning and Characterization of PBP 1C, a Third Member of the
508 Multimodular Class A Penicillin-binding Proteins of *Escherichia coli* *. *Journal of Biological*
509 *Chemistry* **274**, 32031–32039 (1999).
510 15. Johnson, J. G., Spurbeck, R. R., Sandhu, S. K. & Matson, J. S. Genome sequence of Klebsiella
511 pneumoniae urinary tract isolate Top52. *Genome Announcements* **2**, 668–682 (2014).
512 16. Sutaria, D. S. *et al.* First penicillin-binding protein occupancy patterns of - Lactams and -
513 lactamase inhibitors in klebsiella pneumoniae. *Antimicrobial Agents and Chemotherapy* **62**,
514 (2018).
515 17. Kocaoglu, O. & Carlson, E. E. Profiling of β-Lactam Selectivity for Penicillin-Binding Proteins in
516 Escherichia coli Strain DC2. *Antimicrobial Agents and Chemotherapy* **59**, 2785–2790 (2015).
517 18. Sarigul, N., Korkmaz, F. & Kurultak, İ. A New Artificial Urine Protocol to Better Imitate Human
518 Urine. doi:10.1038/s41598-019-56693-4.
519 19. Bush, K. & Jacoby, G. A. Updated functional classification of β-lactamases. *Antimicrobial*
520 *Agents and Chemotherapy* **54**, 969–976 (2010).
521 20. Kannan, G. *et al.* Rapid acid treatment of Escherichia coli: Transcriptomic response and
522 recovery. *BMC Microbiology* **8**, 37 (2008).

523 21. Maurer, L. M., Yohannes, E., Bondurant, S. S., Radmacher, M. & Slonczewski, J. L. pH Regulates
524 Genes for Flagellar Motility, Catabolism, and Oxidative Stress in Escherichia coli K-12. *Journal*
525 *of Bacteriology* **187**, 304–319 (2005).
526 22. Sardis, M. F., Bohrhunter, J. L., Greene, N. G. & Bernhardt, T. G. The LpoA activator is required
527 to stimulate the peptidoglycan polymerase activity of its cognate cell wall synthase PBP1a.
528 *Proc Natl Acad Sci U S A* **118**, e2108894118 (2021).
529 23. Typas, A. *et al.* Regulation of peptidoglycan synthesis by outer-membrane proteins. *Cell* **143**,
530 1097–1109 (2010).
531 24. Typas, A. *et al.* Regulation of peptidoglycan synthesis by outer-membrane proteins. *Cell* **143**,
532 1097–1109 (2010).
533 25. Choi, U., Park, S. H., Lee, H. B., Son, J. E. & Lee, C.-R. Coordinated and Distinct Roles of
534 Peptidoglycan Carboxypeptidases DacC and DacA in Cell Growth and Shape Maintenance
535 under Stress Conditions. *Microbiology Spectrum* **11**, e00014-23 (2023).
536 26. Peters, K. *et al.* The redundancy of peptidoglycan carboxypeptidases ensures robust cell shape
537 maintenance in Escherichia coli. *mBio* **7**, (2016).
538 27. Identification of a penicillin-binding protein 3 homolog, PBP3x, in Pseudomonas aeruginosa:
539 gene cloning and growth phase-dependent expression.
540 https://journals.asm.org/doi/epdf/10.1128/jb.179.5.1490-1496.1997
541 doi:10.1128/jb.179.5.1490-1496.1997.
542 28. Castanheira, S. *et al.* A Specialized Peptidoglycan Synthase Promotes Salmonella Cell Division
543 inside Host Cells. *mBio* **8**, 10.1128/mbio.01685-17 (2017).
544 29. Castanheira, S. & García-del Portillo, F. Evidence of two differentially regulated elongasomes in
545 Salmonella. *Commun Biol* **6**, 923 (2023).

546 30. Sub-Inhibitory Cefsulodin Sensitization of E. coli to β-lactams Is Mediated by PBP1b Inhibition |
547 PLOS One. https://journals.plos.org/plosone/article?id=10.1371/journal.pone.0048598.
548 31. Ramachandran, V. *et al.* Screen for Inhibitors of the Coupled Transglycosylase-Transpeptidase
549 of Peptidoglycan Biosynthesis in Escherichia coli. *Antimicrobial Agents and Chemotherapy* **50**,
550 1425–1432 (2006).
551 32. Curtis, N. A. C., Eisenstadt, R. L., Turner, K. A. & White, A. J. Inhibition of penicillin-binding
552 protein 3 of Escherichia coli K-12. Effects upon growth, viability and outer membrane barrier
553 function. *Journal of Antimicrobial Chemotherapy* **16**, 287–296 (1985).
554 33. Buijs, J., Dofferhoff, A. S. M., Mouton, J. W., Wagenvoort, J. H. T. & van der Meer, J. W. M.
555 Concentration-dependency of β-lactam-induced filament formation in Gram-negative
556 bacteria. *Clinical Microbiology and Infection* **14**, 344–349 (2008).
557 34. Paradis-Bleau, C. *et al.* Lipoprotein Cofactors Located in the Outer Membrane Activate
558 Bacterial Cell Wall Polymerases. *Cell* **143**, 1110–1120 (2010).
559 35. Nichols, R. J. *et al.* Phenotypic Landscape of a Bacterial Cell. *Cell* **144**, 143–156 (2011).
560 36. Boes, A., Olatunji, S., Breukink, E. & Terrak, M. Regulation of the Peptidoglycan Polymerase
561 Activity of PBP1b by Antagonist Actions of the Core Divisome Proteins FtsBLQ and FtsN. *mBio*
562 **10**, 10.1128/mbio.01912-18 (2019).
563 37. Bertsche, U. *et al.* Interaction between two murein (peptidoglycan) synthases, PBP3 and
564 PBP1B, in Escherichia coli. *Molecular microbiology* **61**, 675–690 (2006).
565 38. Castanheira, S. *et al.* An alternative penicillin-binding protein involved in *Salmonella* relapses
566 following ceftriaxone therapy. *eBioMedicine* **55**, 102771 (2020).
567 39. van der Ploeg, R. *et al.* Colocalization and interaction between elongasome and divisome
568 during a preparative cell division phase in scherichia coli. *Molecular Microbiology* **87**, 1074–
569 1087 (2013).

570 40. Castanheira, S., López-Escarpa, D., Paradela, A. & García-del Portillo, F. In Vivo Cross-Linking
571 Sheds Light on the Salmonella Divisome in Which PBP3 and PBP3 Compete for Occupancy.
572 *Molecular Microbiology* **n/a**,.
573 41. Hardy, C. D. Essential Paralogous Proteins as Potential Antibiotic Multitargets in Escherichia
574 coli. *Microbiology Spectrum* **10**, e02043-22 (2022).
575 42. Machen, T. E. & Paradiso, A. M. Regulation of intracellular pH in the stomach. *Annu Rev Physiol*
576 **49**, 19–33 (1987).
577 43. Fallingborg, J. Intraluminal pH of the human gastrointestinal tract. *Dan Med Bull* **46**, 183–196
578 (1999).
579 44. O'Hanlon, D. E., Come, R. A. & Moench, T. R. Vaginal pH measured in vivo: lactobacilli
580 determine pH and lactic acid concentration. *BMC Microbiol* **19**, 13 (2019).
581 45. García-nafría, J., Watson, J. F. & Greger, I. H. OPEN IVA cloning : A single-tube universal cloning
582 system exploiting bacterial In Vivo Assembly. *Nature Publishing Group* 1–12 (2016)
583 doi:10.1038/srep27459.
584 46. Bachman, M. A. *et al*. Genome-wide identification of Klebsiella pneumoniae fitness genes
585 during lung infection. *mBio* **6**, (2015).
586 47. Datsenko, K. A. & Wanner, B. L. One-step inactivation of chromosomal genes in Escherichia
587 coli K-12 using PCR products. *Proceedings of the National Academy of Sciences* **97**, 6640–6645
588 (2000).
589 48. Ducret, A., Quardokus, E. M. & Brun, Y. V. MicrobeJ, a tool for high throughput bacterial cell
590 detection and quantitative analysis. *Nature Microbiology* **1**, 1–7 (2016).
591

592 **Figure Legends**

593 **Fig 1. *Klebsiella pneumoniae* exhibits acid-dependent resistance to Beta-lactams.**

594 (A) Heatmap displaying the fold-change in minimal inhibitory change (MIC) for *K. pneumoniae*
595 TOP52 at indicated pH relative to neutral pH. Each cell represents the median fold-change value
596 from a minimum of three biological replicates performed in LB buffered to indicated pH with MMT
597 buffer. Specific Beta-lactam antibiotics along with their preferential PBP target are indicated on the
598 Y-axis. NS = non-specific (B) The fold-change in Meropenem (MER) or Cephalexin (CEX) MIC of *K.*
599 *pnuemoniae* strains ATCC 43816 and NHUT-K2044 grown at pH 4.8 compared to growth at pH 6.8.
600 Bars represent mean and error bars denote standard deviation. C-D) Representative micrographs
601 of terminal morphologies of *K. pneumoniae* TOP52 following growth for 20 hours in LB (pH 4.8 or
602 6.8) and treated with Meropenem (C) or Cephalexin (D) at indicated concentrations. Scale bar = 2
603 µm.

604 **Fig 2. Loss of either PBP1b or PBP3$_{PARA}$ results in differential impacts to beta-lactam**
605 **resistance at low pH.** (A-D) Fold change in MICs at pH 4.8 relative to pH 6.8 shown for generalist
606 (A), class A-targeting (B), PBP2-targeting (C), and PBP3-targeting (D) beta-lactams. Data are
607 graphed as median values with range. (E) Micrographs from time-lapse microscopy of WT (top) or
608 Δ*mrcB* (bottom) growing in the presence of CEX at low pH. Microscopy pads comprised of LB
609 buffered with MMT to pH 4.8 + 15.6 µg/mL CEX + 1.5 µM propidium iodide + 1% agarose. The CEX
610 concentration reflects the 1X MIC for the Δ*mrcB* mutant and 0.06X MIC for the WT strain.

611 **Fig 3. *Klebsiella pneumoniae* possesses acid-responsive paralogous copies of the Class B**
612 **PBPs.** (A) Genomic regions containing the canonical PBP2, encoded by *mrdA*, and the paralogous
613 gene *mrdA2,* which encodes PBP2$_{PARA}$ (B) Genomic regions containing the canonical PBP3,
614 encoded by *ftsI,* and the paralogous gene *ftsI2,* which encodes PBP3$_{PARA}$. (C & D) Domain
615 conservation between canonical and paralogous copies of PBP2 (C) and PBP3 (D). Domains are
616 denoted as follows: Transmembrane (TM), Lipoprotein lipid attachment site (LP, PS51257) PBP-
617 dimer (Pfam: PF03717), Transpeptidase domain (Pfam: PF00905). The location of motifs that are
618 critical for enzyme catalysis are highlighted in purple.

619 **Fig 4. Loss of PBP3$_{PARA}$ impairs division at low pH.** (A) Representative micrographs of indicated
620 strains following growth in LB buffered to pH 4.8 (top panels) or growth in LB buffered to pH 6.8
621 (bottom panels). For complementation studies with either empty vector (EV) or p*ftsI2,* the media
622 was supplemented with 0.1 mM IPTG. Scale bar = 10 uM. (B-C) Quantification of cell length in (B).
623 Each data point represents the mean of a biological replicate (>50 cells analyzed for each
624 replicate). The bar represents the mean of three biological replicates, and the error bars represent

625 the standard error of the mean. Statistical significance was determined by a one-way ANOVA with
626 Tukey's correction for multiple comparisons with asterisks denoting significance as follows:** =
627 p<0.005, * = p<0.5.

628 **Fig 5. Loss of either PBP1b or PBP3$_{PARA}$ results in differential impacts to Beta-lactam**
629 **resistance at low pH.** (A-D) Fold change in MICs at pH 4.8 relative to pH 6.8 shown for generalist
630 (A), class A-targeting (B),PBP2-targeting (C), and PBP3-targeting Beta-lactams. For comparison,
631 data for MER and CEX are re-graphed from Fig 4. Data are presented as median values with range.
632 (E) Micrographs from time-lapse microscopy of WT, Δ*ftsI2,* Δ*mrdA2,* and Δ*mrdA2* Δ*ftsI2* growing in
633 the presence of MER at low pH. Microscopy pads comprised of LB buffered with MMT to pH 4.8 +
634 0.2 µg/mL MER + 1.5 µM propidium iodide + 1% agarose. The MER concentration reflects 1X MIC for
635 WT, ~0.25X MIC for Δ*ftsI2,* ~2X MIC for Δ*mrdA2*, and ~0.5X MIC for Δ*mrdA2* Δ*ftsI2.*

636

Fig 1

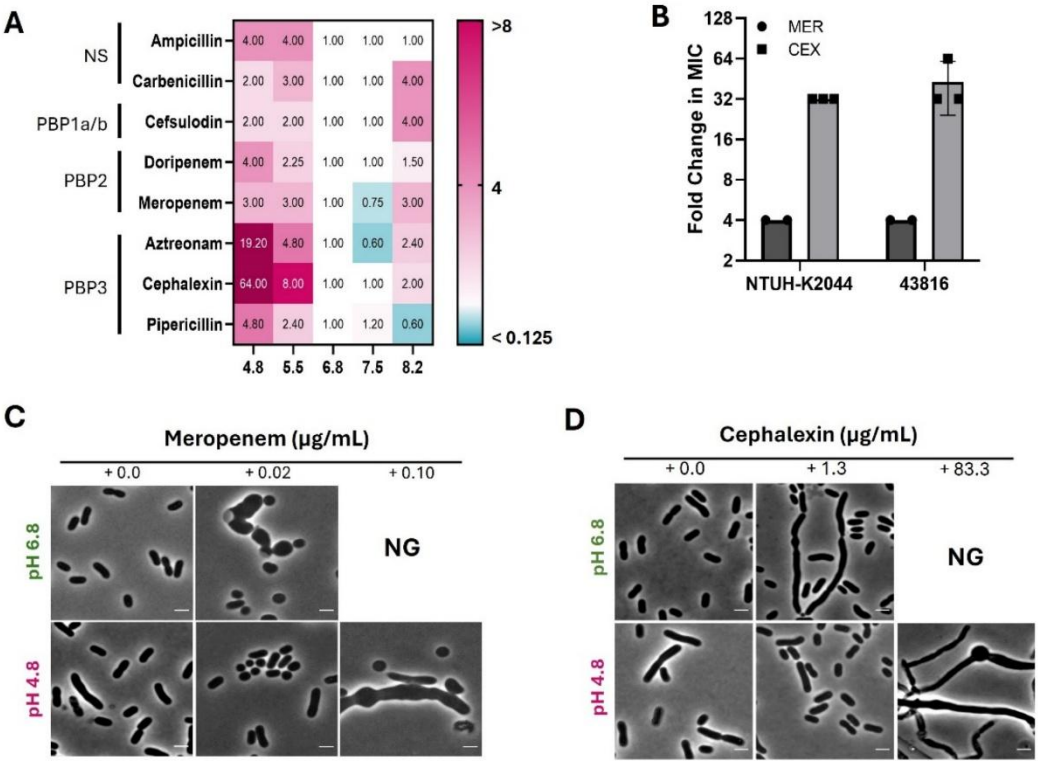
A
NS
Ampicillin
Carbenicillin
PBP1a/b
Cefsulodin
PBP2
Doripenem
Meropenem
PBP3
Aztreonam
Cephalexin
Pipericillin
4.00 4.00 1.00 1.00 1.00
2.00 3.00 1.00 1.00 4.00
2.00 2.00 1.00 1.00 4.00
4.00 2.25 1.00 1.00 1.50
3.00 3.00 1.00 0.75 3.00
19.20 4.80 1.00 0.60 2.40
64.00 8.00 1.00 1.00 2.00
4.80 2.40 1.00 1.20 0.60
4.8 5.5 6.8 7.5 8.2
>8
4
< 0.125
B
MER
CEX
Fold Change in MIC
128
64
32
16
8
4
2
NTUH-K2044
43816
C
Meropenem (μg/mL)
+ 0.0
+ 0.02
+ 0.10
pH 6.8
pH 4.8
NG
D
Cephalexin (μg/mL)
+ 0.0
+ 1.3
+ 83.3
pH 6.8
pH 4.8
NG

637

638

Fig 2

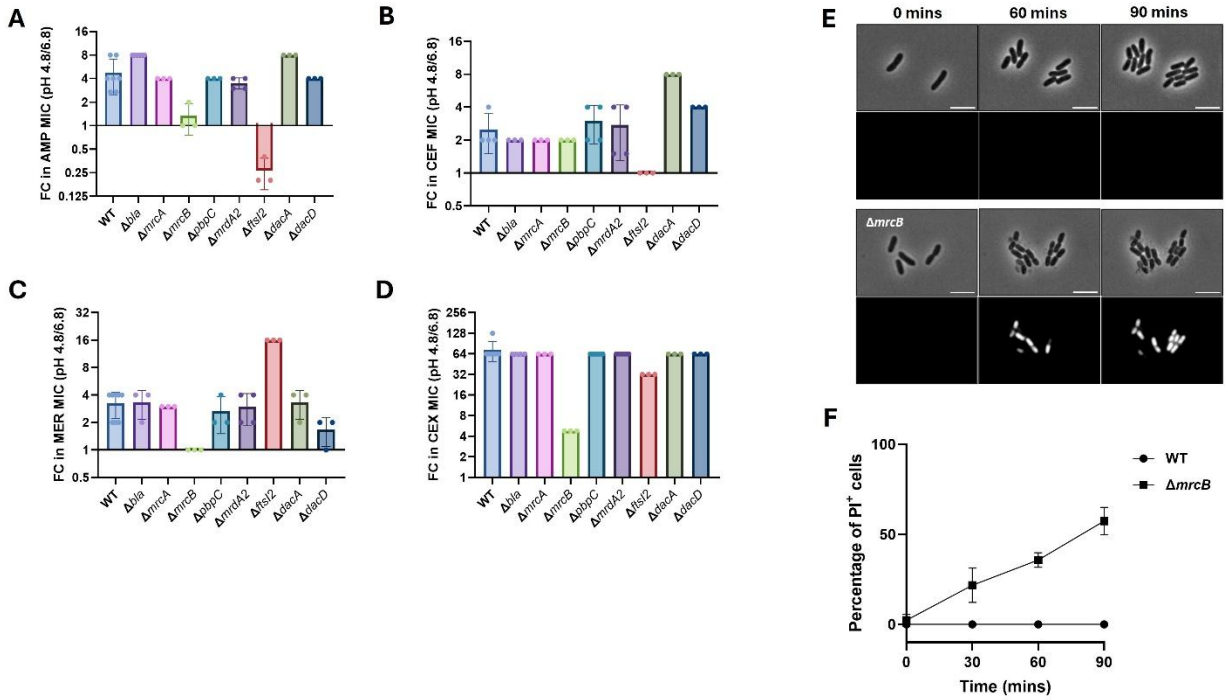
A
FC in AMP MIC (pH 4.8/6.8)
B
FC in CEF MIC (pH 4.8/6.8)
C
FC in MER MIC (pH 4.8/6.8)
D
FC in CEX MIC (pH 4.8/6.8)
WT
Δbla
ΔmrcA
ΔmrcB
ΔpbpC
ΔmrdA2
Δftsl2
ΔdacA
ΔdacD
E
0 mins
60 mins
90 mins
ΔmrcB
F
Percentage of PI+ cells
Time (mins)
WT
ΔmrcB

639

640

Fig 3

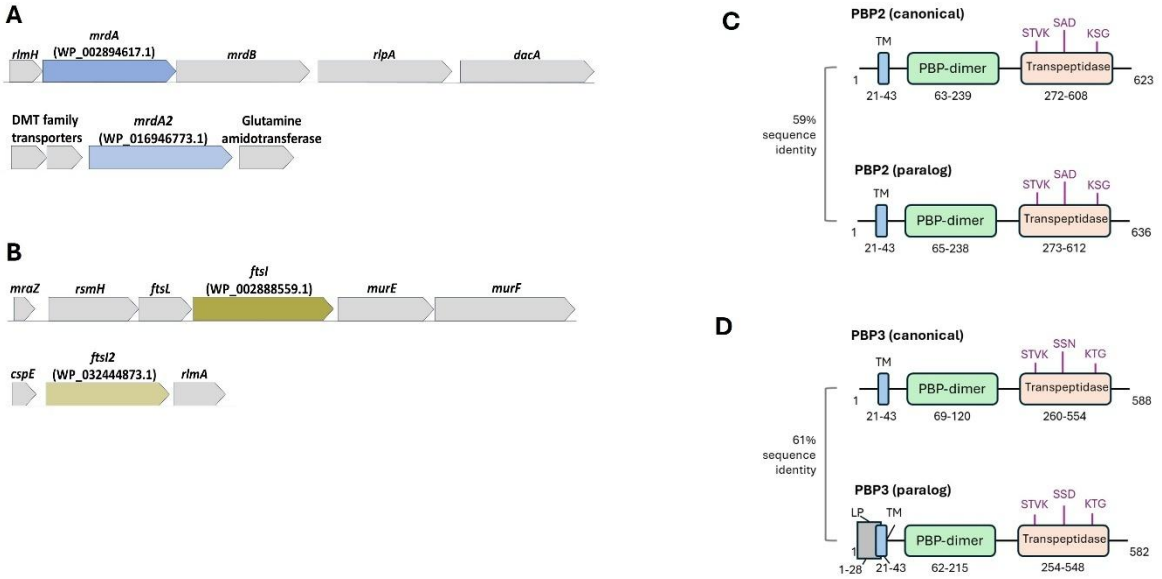

641

642

Fig 4

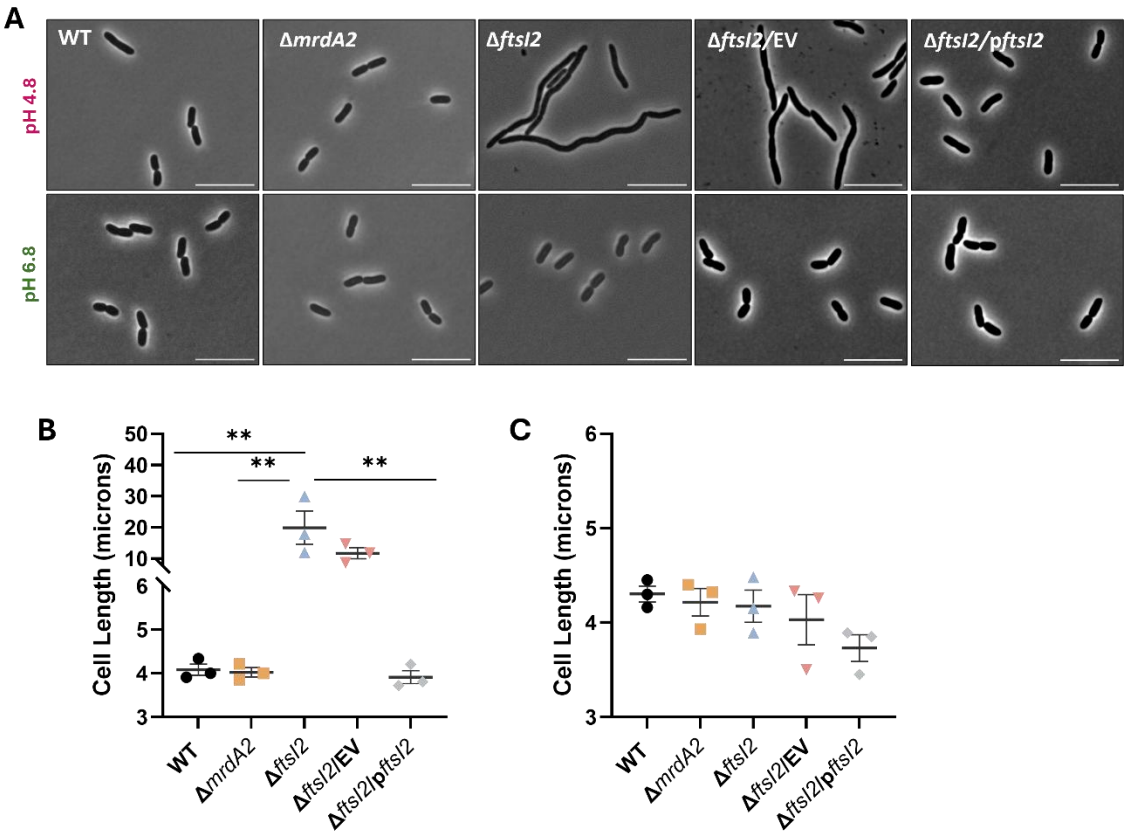
A
WT
ΔmrdA2
ΔftsI2
ΔftsI2/EV
ΔftsI2/pftsI2
pH 4.8
pH 6.8
B
Cell Length (microns)
50
40
30
20
10
6
5
4
3
**
**
**
WT
ΔmrdA2
ΔftsI2
ΔftsI2/EV
ΔftsI2/pftsI2
C
Cell Length (microns)
6
5
4
3
WT
ΔmrdA2
ΔftsI2
ΔftsI2/EV
ΔftsI2/pftsI2

643

644

645

Fig 5

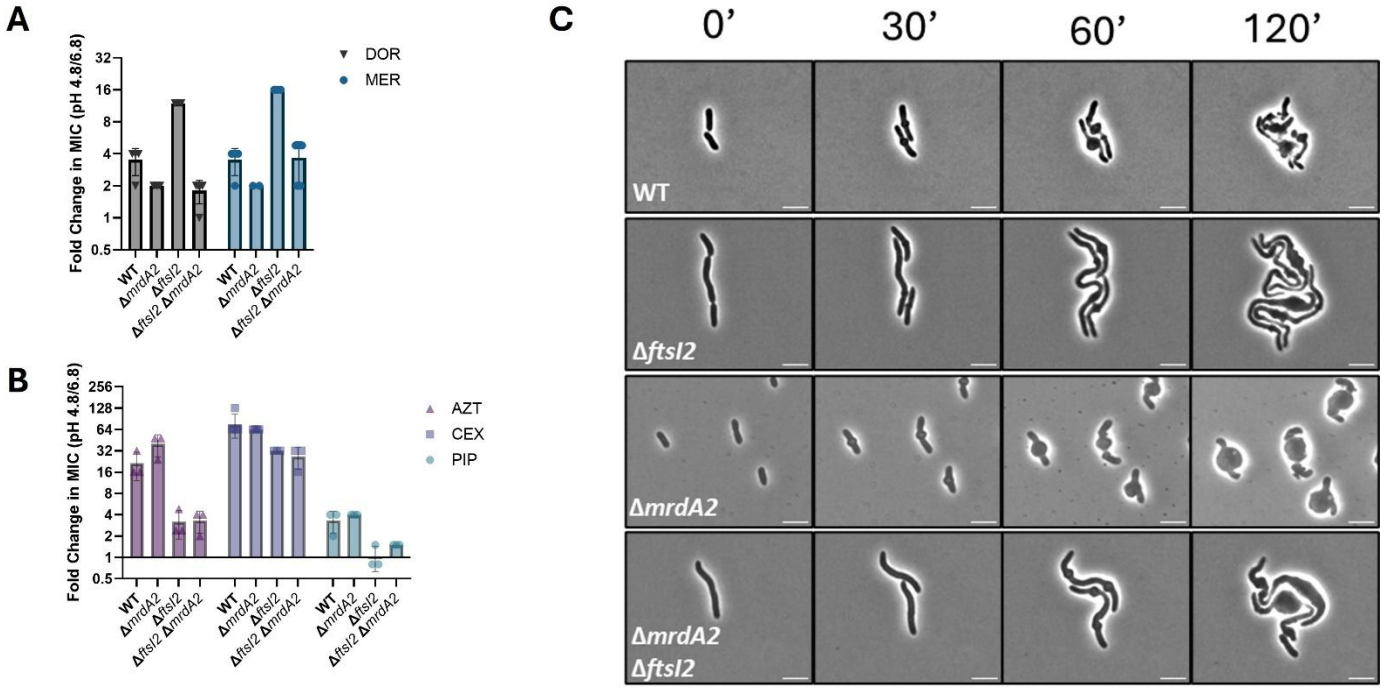
A
Fold Change in MIC (pH 4.8/6.8)
32
16
8
4
2
1
0.5
DOR
MER
WT
ΔmrdA2
ΔftsI2
ΔftsI2 ΔmrdA2
B
256
128
AZT
CEX
PIP
C
0'
30'
60'
120'
WT
ΔftsI2
ΔmrdA2
ΔmrdA2
ΔftsI2

646

647 **Table 1. Transcriptional response to pH of key beta-lactam targets in *K. pneumoniae* and *E.***
648 ***coli***

	Gene	Enzyme Encoded	Description	log_2FC (pH 4.8/6.8)
K. pneumoniae				
D1637_RS05825	*mrcA*	PBP1a	bifunctional glycosyl transferase/transpeptidase	**0.60**
D1637_RS12385	*mrcB*	PBP1b	bifunctional glycosyl transferase/transpeptidase	**-0.39**
D1637_RS01040	*pbpC*	PBP1c	peptidoglycan glycosyltransferase	**-1.61**
D1637_RS15400	*mrdA*	PBP2	canonical peptidoglycan DD-transpeptidase	**0.84**
D1637_RS12000	*ftsI*	PBP3	canonical peptidoglycan DD-transpeptidase	**0.23**
D1637_RS21590	*mrdA2*	$PBP2_{para}$	paralogous peptidoglycan DD-transpeptidase	**3.41**
D1637_RS24275	*ftsI2*	$PBP3_{para}$	paralogous peptidoglycan DD-transpeptidase	**3.28**
D1637_RS15385	*dacA*	PBP5	D-Ala-D-Ala-carboxypeptidase	**1.20**
D1637_RS25010	*dacD*	PBP6b	D-Ala-D-Ala carboxypeptidase	**1.63**
D1637_RS17685	*lpoB*	LpoB	Outer membrane activator of PBP1b	**-1.12**
E. coli				
b3396	*mrcA*	PBP1a	bifunctional glycosyl transferase/transpeptidase	**0.36**
b0149	*mrcB*	PBP1b	bifunctional glycosyl transferase/transpeptidase	**-0.23**
b2519	*pbpC*	PBP1c	peptidoglycan glycosyltransferase	**-0.43**
b0635	*mrdA*	PBP2	canonical peptidoglycan DD-transpeptidase	**0.47**
b0084	*ftsI*	PBP3	canonical peptidoglycan DD-transpeptidase	**-0.64**
b0632	*dacA*	PBP5	D-alanyl-D-alanine carboxypeptidase	**0.95**
b2010	*dacD*	PBP6b	D-alanyl-D-alanine carboxypeptidase	**2.63**
B1105	*LpoB*	LpoB	Outer membrane activator of PBP1b	**-1.33**

649 *Shaded genes represent those that were differentially regulated by pH as determined by our cutoff
650 of |logFC| > 1 and $p < .05$. Blue Log_2FC values indicate that the gene was down-regulated during
651 growth at pH 4.8 versus pH 6.8. Magenta Log_2FC values indicate that the gene was up-regulated
652 during growth at pH 4.8 versus pH 6.8.